

A complex online model for the iron ore reduction in the blast furnace

Y. Kaymak¹, H. Bartusch¹, T. Hauck¹, D.I. Durneata², S. Hojda²

1. Process Optimisation Iron and Steel Making, VDEh-Betriebsforschungsinstitut GmbH, Düsseldorf, Germany.

2. Technologie Roheisenerzeugung, Aktien-Gesellschaft der Dillinger Hüttenwerke, Dillingen/Saar, Germany.

Abstract

A complex multiphysics model has been developed to simulate the reduction of iron ore in the blast furnace (BF) shaft for various operational conditions and charging programs. The model includes heat exchange between gas and burden, reaction heat sources, mass transfer from solid to gas, compressible non-isothermal porous flow, transport of seven solid species and five gas species, coke/ore distribution and burden layer structures in the computation. The shrinking core reaction kinetics has been calibrated by laboratory trials. This model is adopted to Dillinger BF4. Matlab LiveLink Module is used to prepare input and access the operational database (DB). The burden layer structure data is implemented as (1) a 2D polynomial regression function for the burden layer angle, (2) a polynomial regression function for the coke volume fraction and for the burden surface shape. Other process parameters such as ore and blast gas rates as well as their composition are taken from the online process DB. An open-source optimization Levenberg-Marquardt-Algorithm (LMA) [1] has been adopted for the permeability parameter fine-tuning. The main model results are exported as image files, which can be displayed at the control center when a detailed query of an operational state is needed. The influences of various parameters on process sensitivity are also studied and presented.

Keywords: iron ore reduction kinetics, three interface shrinking core model, reacting non-isothermal flow, anisotropic permeability, online blast furnace process model.

Introduction

The blast furnace (BF) is a counter-current moving bed reactor. The coke and ore are alternatively charged at the top and hot air is blasted through tuyeres at the lower furnace wall. Auxiliary fuels (pulverized coal, oil, coke oven gas, hydrogen rich gases, or natural gas) can be injected into the furnace with the blast air from the tuyeres. In front of the tuyere, coke particles and injected fuel react with oxygen in the hot blast air. This generates carbon monoxide and heat needed for the process. The iron-oxides are reduced by CO and H₂ in the hot gas at the upper part of the furnace. A cohesive zone (CZ) forms at the middle height of the furnace as the reduced iron and slag start melting during decent. The molten iron and slag which are generated in this region drop down through the packed bed of coke particles and flow into the bottom of the furnace. Although various mathematical models of the blast furnace have been developed [2] [3] [4] [5] [6] [7] [8] [9] and [10] to simulate the shaft processes, these models are not used as online models for the process monitoring. Present model has an automated input preparation for online monitoring of the process state.

Currently, BF plants have to handle fluctuating raw materials quality, meanwhile trying to achieve the lowest possible coke rates in combination with high pulverized coal injection (PCI) rates. These boundary conditions mutually decrease the permeability and stability of the stack processes, which also dominate the efficiency and safety of the BF process. In this study, innovative measuring techniques, advanced simulation methods and extensive laboratory trials are combined for better process control in the industrial BF plant operation.

Flow through layered packed bed

The burden in the BF has a layered structure. Depending on the charging program, usually more coke is charged towards the center and more ore towards the wall. This charging pattern has a major influence on the permeability distribution and gas flow. Since the coke particles are larger than ore particles, the coke layers have higher permeability than the ore layers. Usually, a burden descent model is used to estimate the shape of the coke and ore layers during the operation with respect to the charging programs and other operational conditions. Since the burden layer structure has a considerable influence, it should be considered in the blast furnace mathematical model. The main challenge is that a high-resolution mesh is required to geometrically resolve the individual layers, which is not suitable for online application. This challenge is overcome by an anisotropic permeability model, which considers different permeabilities in parallel and perpendicular to the layer directions. With this approach, the orientation angle of coke/ore layer as well as the coke/ore volume ratio can be packed into an anisotropic permeability tensor. A similar approach has been suggested in [2]. In general, the particle diameter defines the packed bed permeability via Ergun's equation. The ore/coke volume ratio is a position dependent function at the ore inlet. The mean burden porosity would be simply the arithmetic mean porosity. However, there will be two different permeabilities depending on the flow direction with respect to layer orientation. For the component of the flow direction parallel to the layers, the arithmetic mean permeability of coke and ore layers is valid. For the component of the flow direction perpendicular to the layers, the harmonic mean

permeability is valid. Based on this concept and the chosen coordinate system, a tensor form of permeability is defined in **Table 1**.

Table 1: Burden characteristics and anisotropy which influence the gas flow and heat exchange.

Name	Expression	Unit	Description
fsf	parhsf		flow shape factor for pressure drop calibration
Kdo	$\text{epsln}^3 \cdot (\text{dop} \cdot \text{fsf})^2 / (150 \cdot (1 - \text{epsln})^2)$	m ²	ore layer Darcy permeability
Kdc	$\text{epscl}^3 \cdot (\text{dcp} \cdot \text{fsf})^2 / (150 \cdot (1 - \text{epscl})^2)$	m ²	coke layer Darcy permeability
Kda	$\text{Vo} \cdot \text{Kdo} + \text{Vc} \cdot \text{Kdc}$	m ²	parallel direction Darcy permeability
Kdh	$1 / (\text{Vo} / \text{Kdo} + \text{Vc} / \text{Kdc})$	m ²	perpendicular direction Darcy permeability
tA	bsR(r,z)		$\tan(\text{BurdenSlope}) \cdot dz/dr$
cA	$1 / \sqrt{1 + tA^2}$		$\sin(\text{BurdenSlope})$
sA	$tA / \sqrt{1 + tA^2}$		$\cos(\text{BurdenSlope})$
Kdr	$cA^2 \cdot cA \cdot \text{Kda} + sA^2 \cdot sA \cdot \text{Kdh}$	m ²	rr-component of permeability
Kdrz	$cA \cdot sA \cdot \text{Kda} - cA \cdot sA \cdot \text{Kdh}$	m ²	rz-component of permeability
Kdz	$sA^2 \cdot sA \cdot \text{Kda} + cA^2 \cdot cA \cdot \text{Kdh}$	m ²	zz-component of permeability
Da	$(\text{Vo} + \text{Vc}) / (\text{Vo} / \text{dop} + \text{Vc} / \text{dcp})$	m	average solid particle diameter
epsln	$(\text{Vo} \cdot \text{epsln} + \text{Vc} \cdot \text{epscl}) / (\text{Vo} + \text{Vc})$		average solid voidage
Kd	$\text{epsln}^3 \cdot (\text{Da} \cdot \text{fsf})^2 / (150 \cdot (1 - \text{epsln})^2)$	m ²	Permeability in Forchheimer coeff.
Cf	$1.75 \cdot \text{rhoG} / \sqrt{\text{Da} \cdot \text{fsf} \cdot \text{epsln}^3}$	kg/m ³	Forchheimer Coeff.
r_p	$0.5 \cdot \text{Da} \cdot \text{parhsf}$	m	Particle radius for heat transfer
a_sf	$3 \cdot (1 - \text{epsln}) / r_p$	1/m	Specific surface area
Pr	$\text{max}(\text{muG} \cdot \text{CpG} / \text{K}, \text{eps})$		Prandtl number
Re_p	$\text{max}(2 \cdot \text{rhoG} \cdot \text{Ug} \cdot r_p / (1 - \text{epsln}) \cdot \text{muG}, \text{eps})$		Particle Reynolds number
Nu	$2 \cdot \text{epsln} / (1 - \text{epsln}) + \sqrt{\text{Re}_p} + 0.005 \cdot \text{Re}_p$		Nusselt number
hsg	$\text{Nu} \cdot \text{KG} / (2 \cdot r_p)$	W/(m ² ·K)	Interstitial heat transfer coefficient
qsg	$a_{sf} \cdot hsg$	W/(m ³ ·K)	Interstitial convective heat transfer coefficient
Qsg	$qsg \cdot (T_s - T_g)$	W/m ³	heat exchange between has and solid
KdoCZ	$\text{epsln}^3 \cdot (\text{dop} \cdot \text{fsf})^2 / (150 \cdot (1 - \text{epsln})^2) \cdot 0.05$	m ²	CZ reduced ore permeability
KdcCZ	$\text{epscl}^3 \cdot (\text{dcp} \cdot \text{fsf})^2 / (150 \cdot (1 - \text{epscl})^2) \cdot 0.75$	m ²	CZ reduced coke permeability
KdaCZ	$\text{Vo} \cdot \text{KdoCZ} + \text{Vc} \cdot \text{KdcCZ}$	m ²	CZ perm. parallel to layers
KdhCZ	$1 / (\text{Vo} / \text{KdoCZ} + \text{Vc} / \text{KdcCZ})$	m ²	CZ parm. perpendicular to layers
KdrCZ	$cA^2 \cdot cA \cdot \text{KdaCZ} + sA^2 \cdot sA \cdot \text{KdhCZ}$	m ²	CZ rr-permeability
KdrzCZ	$cA \cdot sA \cdot \text{KdaCZ} - cA \cdot sA \cdot \text{KdhCZ}$	m ²	CZ rz-permeability
KdzCZ	$sA^2 \cdot sA \cdot \text{KdaCZ} + cA^2 \cdot cA \cdot \text{KdhCZ}$	m ²	CZ zz-permeability
epslnCZ	$\text{epscl} \cdot \text{Vc}$		CZ porosity
KdCZ	$\text{epslnCZ}^3 \cdot (\text{dcp} \cdot \text{fsf})^2 / (150 \cdot (1 - \text{epslnCZ})^2)$	m ²	CZ permeability
CF CZ	$1.75 \cdot \text{rhoG} / \sqrt{\text{Da} \cdot \text{fsf} \cdot \text{epslnCZ}^3}$	kg/m ³	CZ Forchheimer coeff.

Table 2: Anisotropic permeability tensor (left table) and its curvilinear base coordinate system (right table).

User defined			Input method:	In-plane base vectors
Kdr	0	Kdrz	Out-of-plane index:	2
0	Kda	0		
Kdrz	0	Kdz		

r	z
$x1 \cdot 1 / \sqrt{1 + \text{bsR}(r,z)} \cdot \text{bsR}(r,z)$	$\text{bsR}(r,z) / \sqrt{1 + \text{bsR}(r,z)} \cdot \text{bsR}(r,z)$
$x3 \cdot \text{bsR}(r,z) / \sqrt{1 + \text{bsR}(r,z)} \cdot \text{bsR}(r,z)$	$1 / \sqrt{1 + \text{bsR}(r,z)} \cdot \text{bsR}(r,z)$

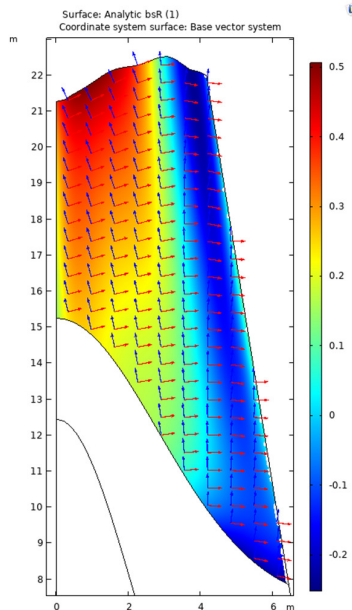


Figure 1. 2D polynomial fitting of the layer orientations for a typical burden layer structure.

The slope of the coke/ore layer as well as the coke/ore volume ratio can be packed into an aniso-

tropic permeability tensor. The permeability tensor and its reference base coordinate system are given in **Table 2**. The form of the 2D regression polynomial for the burden layer angle is “ $\text{bsR}(r,z) = c_{00} + c_{10}r + c_{01}z + c_{20}r^2 + c_{11}rz + c_{02}z^2 + c_{30}r^3 + c_{21}r^2z + c_{12}rz^2 + c_{03}z^3 + \dots$ ”. Similarly, the form of the regression polynomial for the coke volume fraction and for burden surface geometry is “ $\text{Vc}(r) = c_0 + c_1r + c_2r^2 + c_3r^3 + \dots$ ”. For a given burden layer data (e.g., a list of r and z coordinates of discretized layer boundary lines), the coefficients in the regression function for the burden layer angle can be calculated. The comparison of layer angles from the 2D polynomial fit is plotted as contours overlaying on the curvilinear coordinate system in Figure 1.

Heat and mass exchange in BF

The BF shaft is a huge counter-current moving bed reactor in which the heat and mass exchange play a significant role in its mathematical modelling. The heat exchange model is readily available in Comsol Multiphysics® via Local Thermal Non-Equilibrium Interface. This multiphysics coupling is used to account for heat transfer in porous domains, where the solid and gas temperatures are not in equilibrium. This is achieved by coupling the heat equations in the solid and fluid subdomains through a transfer term proportional to the temperature difference between the fluid and the solid. For further details please refer to the software’s heat transfer user guide. An approach with predefined interstitial convective heat transfer coefficient for spherical pellet bed is ideally suited for the situation in blast furnace shaft. In the general configuration, the interstitial convective heat transfer can be directly expressed in terms of the mean specific surface area per unit volume “ a_{sf} ” and the interstitial heat transfer coefficient “ hsg ” which are shown in **Table 1**. The heat transfer between the gas and the burden is calibrated by the shape factor “ $parhsf$ ”, which scales the particle radius “ r_p ” for the heat transfer.

The ore layers lose mass due to oxygen removal as the ore is reduced by CO or H₂. It is assumed that the particle volumes stay constant, and the density is reduced by the increased inter particle porosity of the ore particles. The coke layers also lose mass as the coke reacts with CO₂ to form CO by the solution-loss (Boudouard) reaction. Again, the particle size is assumed to stay constant. The reaction kinetics will be discussed in detail on the subsequent section. The mass source expression can be explicitly defined in the porous flow (in the gas phase). The mass removal from the solid phase means the density reduction for the ore and coke particles. Therefore, the density is solved as an additional variable using the general PDE interface in Comsol for the overall burden.

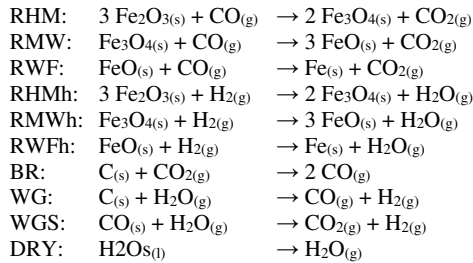
Reaction kinetics models in BF shaft

There are countless reactions occurring in the blast furnace shaft as the burden descends. However, many of these reactions have negligible effects on the ore

reduction process. The most important reactions are the reduction of the ore by CO/H₂ and the solution-loss reaction. So, the unreacted shrinking core model (USCM) is used for these heterogeneous reactions. The overall process proceeds through a sequence of mass transport and chemical reaction steps. The reacted solid product forms a thickening shell as the unreacted core shrinks. Usually, the transport resistance through the interface has a non-negligible influence on the overall kinetics. The theoretical and experimental backgrounds of these models have been founded long back. A thorough insight of these models can be achieved through the following papers [4] [5] [6] and [11].

The transport of solid species and gas species are also readily available in Comsol's Chemical Reaction Engineering Module. It is only necessary to define the reaction source terms for each species. These source terms for solid and gas species are shown in **Table 3**. The software Comsol Multiphysics® provides all the needed functionality to efficiently implement a BF process model.

The complex kinetics expression for each reaction (e.g., ore reduction or solution-loss reaction) can be directly written as sequence of expression in Comsol Multiphysics®. Note that the ore reduction rates are defined at the ore particle level, so they are multiplied by the number of ore particles per unit volume (Nop). Similarly, the coke related reaction rates are defined at coke particle level, so they are multiplied by the number of coke particles per unit volume (Ncp). On the other hand, water-gas-shift (WGS) reaction and evaporation rates are defined at unit bulk volume. All the reaction rates are expressed in terms of mol/(m³·s) so they are multiplied with the respective molar weight to get mass rate. The following reactions, which include seven solid species (Fe₂O₃, Fe₃O₄, FeO, Fe, C, H₂O_s, Slg) and five gas species (CO, CO₂, H₂, H₂O, N₂) are considered in the current state of the model:



The iron ore (H: Hematite) is first reduced to Magnetite (M), then Wüstite (W), and finally metallic iron (F) in three steps. The reducing gases (CO / H₂) are transported by diffusion to the reaction interface. Therefore, at an intermediate state, the ore particle may contain hematite (Fe₂O₃), magnetite (Fe₃O₄), wüstite (FeO) and iron (Fe) layers from core towards its surface. The derivation of the reaction kinetics in terms of USCM is very nicely described by [4] and [5]. The coke gasification by Boudouard and water gas (WG) reaction kinetics are also modelled in terms of USCM. These kinetic equations are taken

from reference (see [7]). The water gas shift (WGS) reaction is a homogeneous reaction among gas species, and it is quite fast. Its kinetics equation is taken from references [7] and [8]. The evaporation/condensation of the moisture (DRY) in ore and coke happens at the very upper part of the burden.

Table 3: Reaction source terms for each solid and gas species in the transport equations.

R _{wFe2O3}	-3*(RHM+RHMh)*Nop*M_Fe2O3
R _{wFe3O4}	2*(RHM+RHMh)-(RMW+RMWh)*Nop*M_Fe3O4
R _{wFeO}	3*(RMW+RMWh)-(RWF+RWFh)*Nop*M_FeO
R _{wFe}	(RWF+RWFh)*Nop*M_Fe
R _{wC}	-(BR+WG)*Ncp*M_C
R _{wSlg}	0
R _{wH2Os}	-DRY*M_H2O
R _{wCO}	-(RHM+RMW+RWF)*Nop+(2*BR+WG)*Ncp-WGS)*M_CO
R _{wCO2}	((RHM+RMW+RWF)*Nop-BR*Ncp+WGS)*M_CO2
R _{wH2}	-(RHMh+RMWh+RWFh)*Nop+WG*Ncp+WGS)*M_H2
R _{wH2O}	((RHMh+RMWh+RWFh)*Nop-WG*Ncp-WGS+DRY)*M_H2O
R _{wN2}	0

Calibration of reaction kinetics parameters

A series of isothermal reduction experiments on the sinter and pellets have been performed to calibrate reaction kinetics [12] and [13]. At each isothermal temperature, six gas-mixture programs are used. That means three programs with the gas composition (CO + CO₂ + N₂) corresponding BF center, wall, and average conditions. Additionally, the same three programs with gas compositions (CO + CO₂ + N₂ + H₂ + H₂O). For example, the determination of reaction kinetic equations for hematite → magnetite (HM), magnetite → wüstite (MW) and wüstite → iron (WM) can be done using a simple optimization in which the measured isothermal reduction degree (RD) curve is fitted by changing three reaction rates. Once the isothermal reaction rates (i.e., the circles in Figure 2) are obtained, the temperature dependent Arrhenius form can be obtained by weighted linear fits to these data. The calibrated kinetic equations are compatible with those reported in [6] and [9].

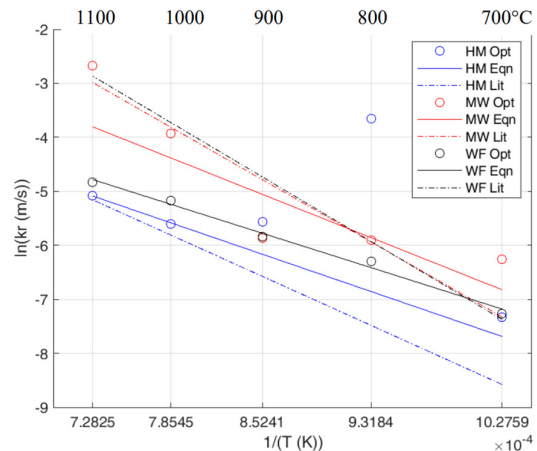


Figure 2. Calibration of the sinter reduction kinetic parameters.

Influence of cohesive zone

The scope of the current model covers the heat and mass transfer as well as reactions above the cohesive zone (CZ). None the less, the gas flow in the complete blast furnace above the tuyeres is solved to have a realistic gas inflow condition at the upper boundary of the CZ. The ore and coke layer permeabilities are reduced at the CZ by factor 0.03 and 0.75, respectively, as shown in **Table 1**. These scale factors give good match to the measured gas pressure at the wall as shown in Figure 3. It is assumed that only coke remains in the so-called deadman (DM) region below the CZ so only coke layer properties are used for the deadman. The shape of the upper and lower boundaries of the CZ is described by a Gaussian curve, e.g., $A \cdot \exp(-(r/B)^2)$, where A and B define the height and flatness, respectively. The influence of the CZ shape on the process is also studied by changing A and B values in the parameter sensitivity study.

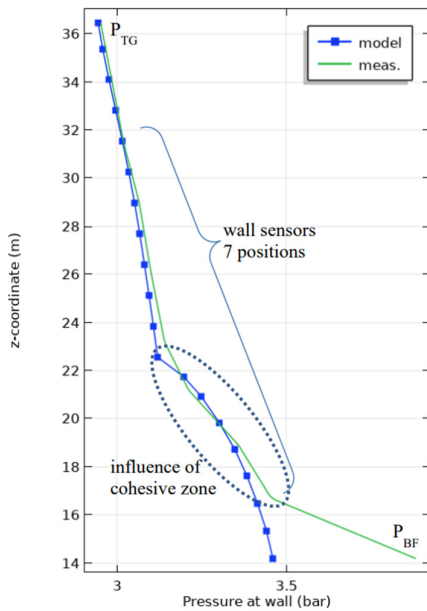


Figure 3. Calibration of the burden permeability (e.g., flow shape factors fsf) to fit the measured gas pressures at the wall.

Connection to online process DB

The main operational data which are connected to the online stack model are the following: (1) hot blast volume, (2) burden chemical composition, (3) burden depth / decent velocity, (4) production of hot metal and slag, (5) gas temperature and composition along in-burden probes, (6) gas pressure on the wall, (7) 2D top gas temperature, (8) gas temperature at uptake, and (9) 2D axi-symmetric burden layer data. Most of these data is stored in a SQL based DB as time-series except for the 2D top gas temperature profile (SOMA) [14] and burden structure data. The SOMA data can be obtained using a simple Matlab script which utilizes the built-in “webread” function. The query URL syntax is supply by the SOMA system producer. The burden layer structure is computed by Dillinger in-house code using the charging

program data [15]. All these data are directly or indirectly fed into the model so that the model represents the current operational state of the BF.

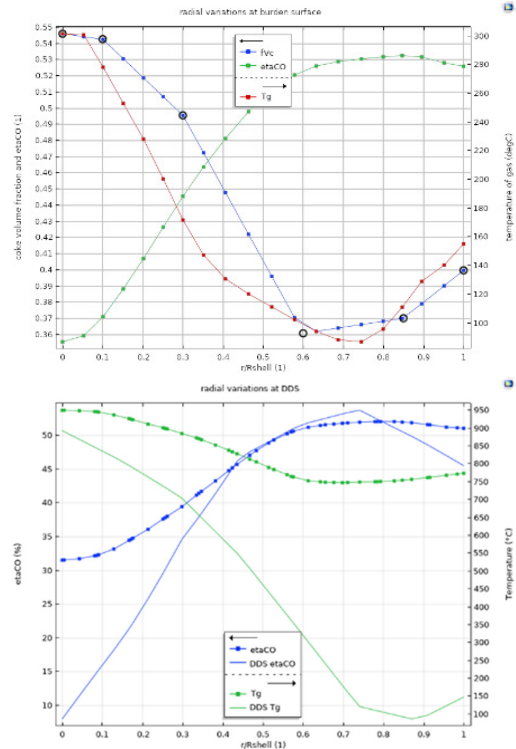


Figure 4. Radial variation of top gas temperature, CO utilization, feed coke volume fraction as in upper plot; comparison of gas temperature and CO utilization in-burden probe and simulation as in lower plot.

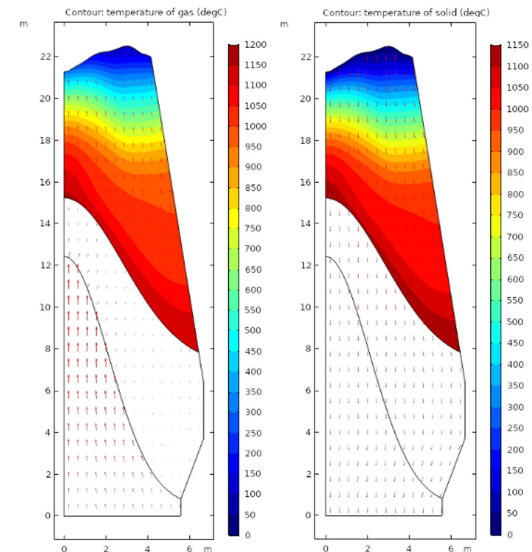


Figure 5. Gas and solid temperature contours in the reaction zone.

Several optimization algorithms are available in reference [1]. The Levenberg-Marquardt-Algorithm (LMA) has been adopted for parameter optimizations. The optimization function is a straightforward Matlab script in which the Comsol model file is first

loaded, then the needed parameters are updated, and then the model is solved. Finally, the needed results are returned. Gas flow related parameters “parVg” (which fine tunes the gas flow rate) and “parfsf” (which fine-tunes the permeability) are fitted to measured molar flow rate of non-reacting N₂ and measured wall pressure distribution. By this way, realistic gas flow rates are obtained without modeling the raceway phenomena. The main model results (e.g., the radial variation of top gas temperature, CO utilization, feed coke volume fraction as in upper plot in Figure 4, comparison of gas temperature and CO utilization in-burden probe and simulation as in lower plot in Figure 4, or gas and solid temperature contours as in Figure 5) are exported as image files, which can be displayed at the control center when a detailed query of an operational state is needed.

Parameter sensitivity study

Seven different model parameters, which are listed in Table 4, are individually varied keeping other operational conditions unchanged. Although the model parameters cannot be changed independently, for example, the blast gas rate must be increased to increase the production rate, or it is not easy to change bed permeability. Two different CZ shapes are compared to find the correlation to the top gas temperature measurement by SOMA. In addition to CZ shape, hot gas inflow rate, top gas pressure, burden permeability, hot metal production rate, and coke volume ratio distributions are studied.

Table 4: Model parameters for sensitivity analysis.

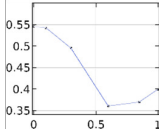
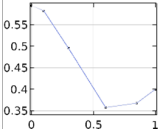
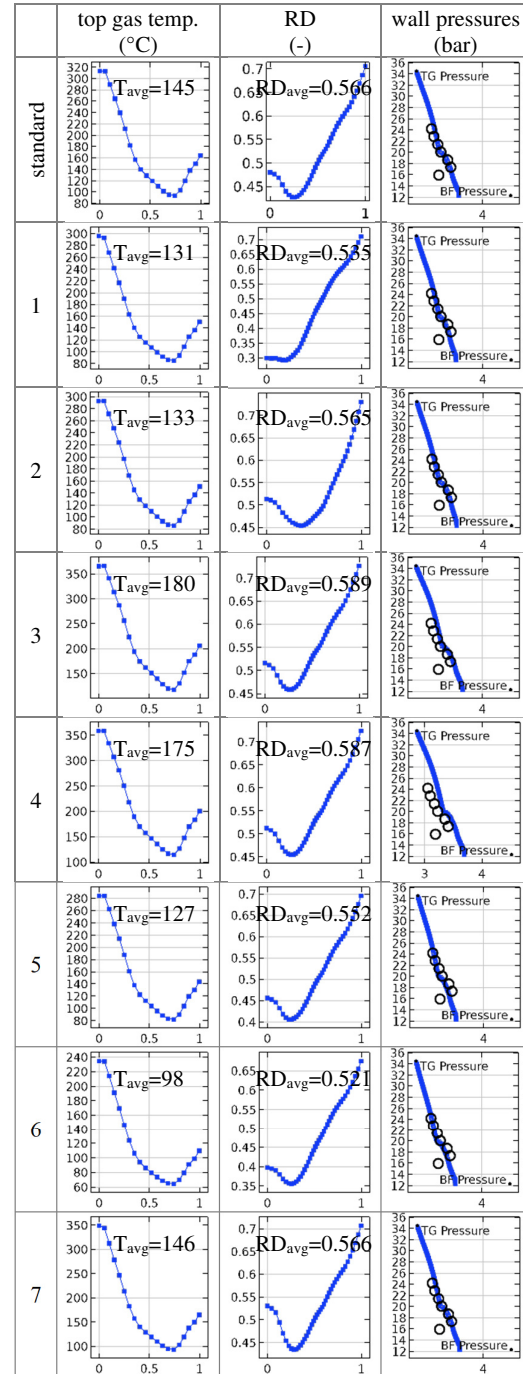
Varied Parameters	Standard Values	Changed Value
1) CZ height, (i.e., coef. A in $A \cdot \exp(-(r/B)^2)$)	12 m 8 m	14 m 10 m
2) CZ flatness; (i.e., coef. B in $A \cdot \exp(-(r/B)^2)$)	4 m 3 m	5 m 3.75 m
3) Hot gas inflow rate (parVg)	1.33 m/s	1.36 m/s
4) Top gas pressure (P _{tg})	1.76 bar	1.85 bar
5) Burden permeability calibration parameter (parfsf)	0.60	0.63
6) Production rate	6487 t/day	6750 t/day
7) Coke volume ratio (fVc)		

Table 5: Comparison of the results for different parameter combinations according to Table 3. The top gas temperature, reduction degree, and wall pressure are plotted against the dimensionless radius of the furnace.



The main results of the model are the top gas temperature profile, reduction degree (RD), and wall pressure measurements. The wall pressure results reveal that the flatness of the CZ has no remarkable influence on the dry stack wall pressure (upper part of the shaft). The pressure increase behaviors in the CZ area (lower part of the shaft) are slightly different. Though, the pressure is mostly controlled by the distance through CZ from DM to the wall. Therefore,

the pressure drop is steeper for the low CZ shape (left figure) where the wall distance to deadman is higher.

The top gas temperatures are quite sensitive to the model parameters. Even the lastly charged burden layers redirect and cool-down the through flowing gas, which is also seen in the SOMA when the charging program and the coke/ore ratio distribution are changed. The main parameters controlling the wall pressure distribution are the bed permeability and gas flow rate.

Summary and Conclusions

In this study, a new stack process model has been developed to study the relation between the CZ properties and operational measurements performed at the BF wall and top. Reaction non-isothermal flow through the layered packed bed model is discussed. The heat and mass exchange phenomena above the CZ are discussed. The calibration of heat transfer from gas to burden is explained. Also, the reduction of burden density due to mass transfer is described by assuming unchanging particle volumes. The reaction kinetics models are mentioned. In total, ten reactions are modelled. For the solid-gas reactions, the unreacted-shrinking core models (USCM) have been adapted. The calibrations of the reaction kinetic parameters are based on experimental results. The influences of dry burden and CZ parameters on the dry stack process simulation is investigated. The CZ and deadman are included only for the flow without reactions and heat and mass exchange. The calibration of the CZ permeability to the measured wall (stave) pressures is explained. The influences of different CZ shapes on the wall pressure and top gas temperature are discussed.

Comsol Multiphysics® software has been successfully applied to model the complex BF process for the reduction of iron ore. The model includes heat exchange between gas and burden, reaction heat sources, mass transfer from solid to gas, compressible non-isothermal porous flow, transport of solid and gas species, coke/ore distribution and burden layer structures in the computation. The USCM reaction kinetics has been calibrated by laboratory trials. This model is adopted to Dillinger BF4. Matlab LiveLink Module is used to prepare input and access the operational DB.

References

- [1] H. B. Nielsen, "immoptibox: a Matlab toolbox for optimization and data fitting," 2010.
- [2] H. Rausch, S. Böhnisch and D. Sert, "Extended blast furnace permeability monitoring," EU, 2006.
- [3] H. Nogami, M. Chu and J. Yagi, "Numerical analysis on blast furnace performance with novel feed material by multi-dimensional simulator based on multi-fluid theory," *Applied Mathematical Modelling*, vol. 30, pp. 1214-, 2006.
- [4] H. Spitzer, F. S. Manning and W. O. Philbrook, "Generalized Model for the Gaseous, Topochemical Reduction of Porous Hematite Spheres," *Transactions of the Metallurgical Society of AIME*, vol. 236, pp. 1715-1724, 1966.
- [5] H. Spitzer, F. S. Manning and W. O. Philbrook, "Mixed-Control Reaction Kinetics in the Gaseous Reduction of Hematite," *Transactions of the Metallurgical Society of AIME*, vol. 236, pp. 726-742, 1966.
- [6] I. Muchi, "Mathematical Model of Blast Furnace," *Transactions ISIJ*, vol. 7, pp. 223-237, 1967.
- [7] ISIJ, Blast furnace phenomena and modelling, London and New York: Elsevier applied science, 1987.
- [8] N. Miyasaka, M. Sugata, Y. Hara and S. Kondo, "Prediction of Blast Pressure Change by a Mathematical Model," *Trans. ISIJ*, vol. 15, pp. 27-36, 1975.
- [9] T. Murayama, Y. Ono and Y. Kawai, "Step-wise Reduction of Hematite Pellets with CO-CO₂ Gas Mixtures," *Tetsu-to-Hagané*, vol. 63, pp. 1099-1107, 1977.
- [10] F. Mauret, M. Baniyasi, H. Saxen, A. Feiterna and S. Hojda, "Impact of Hydrogenous Gas Injection on the Blast Furnace Process: A Numerical Investigation," *Metallurgical and Materials Transactions B*, vol. 54, no. August 2023, pp. 2137-2158, 2023.
- [11] T. Yagi and Y. Ono, "A Method of Analysis for Reduction of Iron Oxide in Mixed-Control Kinetics," *Transactions ISIJ*, vol. 8, pp. 377-381, 1968.
- [12] A. M. Heikkilä, A. M. Koskela, M. O. Iljana, R. Lin, H. Bartusch, E.-P. Heikkinen and T. M. J. Fabritius, "Coke Gasification in Blast Furnace Shaft Conditions with H₂ and H₂O Containing Atmospheres," *Steel Research International*, vol. 92, no. 3, 2020.
- [13] A. Heikkilä, M. Iljana, H. Bartusch and T. Fabritius, "Reduction of Iron Ore Pellets, Sinter, and Lump Ore under Simulated Blast Furnace Conditions," *Steel Research International*, vol. 91, no. 11, 2020.
- [14] M. Tonteling, M. Brodeck and H. Rausch, "2D Blast Furnace Top Gas Temperature Measurement System - TMT SOMA," *Iron & Steel Technology*, vol. 12, pp. 45-55, 2013.
- [15] S. Hojda, M. Pollet, H. Busch, R. Lin, K. Amend and F. Rückert, "Real Time Modelling of Burden Components Distribution During Hopper Outflow and Burdening Via a Rotating Chute," *BHM*

Berg- und Hüttenmännische Monatshefte,
vol. 167, no. 3, pp. 107 - 113, 2022.

Acknowledgements

The work presented here has been conducted with a financial grant from the Research Fund for Coal and Steel (RFCS) of the European Community with Grant Agreement No: 709816 and project title "Online Blast Furnace Stack Status Monitoring" (StackMonitor).